



Tree Physiology 43, 441–451
<https://doi.org/10.1093/treephys/tpac133>



Research paper

Esca grapevine disease involves leaf hydraulic failure and represents a unique premature senescence process

Giovanni Bortolami ^{1,2}, Nathalie Ferrer¹, Kendra Baumgartner³, Sylvain Delzon⁴, David Gramaje ⁵, Laurent J. Lamarque ^{4,6}, Gianfranco Romanazzi ⁷, Gregory A. Gambetta ⁸ and Chloé E.L. Delmas ^{1,9}

¹INRAE, BSA, ISVV, SAVE, 33882 Villenave d'Ornon, France; ²Naturalis Biodiversity Center, PO Box 9517, 2300 RA Leiden, The Netherlands; ³United States Department of Agriculture-Agricultural Research Service, Crops Pathology and Genetics Research Unit, Davis, CA 95616, USA; ⁴Univ. Bordeaux, INRAE, BIOGECO, 33615 Pessac, France; ⁵Institute of Grapevine and Wine Sciences (ICVV), Spanish National Research Council (CSIC), University of La Rioja and Government of La Rioja, Logroño 26007, Spain; ⁶Département des Sciences de l'Environnement, Université du Québec à Trois-Rivières, Trois-Rivières, Québec, G9A 5H7, Canada; ⁷Department of Agricultural, Food and Environmental Sciences, Marche Polytechnic University, Ancona, Italy; ⁸EGFV, Bordeaux-Sciences Agro, INRAE, Université de Bordeaux, ISVV, 33882 Villenave d'Ornon, France; ⁹Corresponding author (chloe.delmas@inrae.fr)

Received February 21, 2022; accepted November 16, 2022; handling Editor Henry Adams

Xylem anatomy may change in response to environmental or biotic stresses. Vascular occlusion, an anatomical modification of mature xylem, contributes to plant resistance and susceptibility to different stresses. In woody organs, xylem occlusions have been examined as part of the senescence process, but their presence and function in leaves remain obscure. In grapevine, many stresses are associated with premature leaf senescence inducing discolorations and scorched tissue in leaves. However, we still do not know whether the leaf senescence process follows the same sequence of physiological events and whether leaf xylem anatomy is affected in similar ways. In this study, we quantified vascular occlusions in midribs from leaves with symptoms of the grapevine disease esca, magnesium deficiency and autumn senescence. We found higher amounts of vascular occlusions in leaves with esca symptoms (in 27% of xylem vessels on average), whereas the leaves with other symptoms (as well as the asymptomatic controls) had far fewer occlusions (in 3% of vessels). Therefore, we assessed the relationship between xylem occlusions and esca leaf symptoms in four different countries (California in the USA, France, Italy and Spain) and eight different cultivars. We monitored the plants over the course of the growing season, confirming that vascular occlusions do not evolve with symptom age. Finally, we investigated the hydraulic integrity of leaf xylem vessels by optical visualization of embolism propagation during dehydration. We found that the occlusions lead to hydraulic dysfunction mainly in the peripheral veins compared with the midribs in esca symptomatic leaves. These results open new perspectives on the role of vascular occlusions during the leaf senescence process, highlighting the uniqueness of esca leaf symptoms and its consequence on leaf physiology.

Keywords: hydraulic failure, magnesium deficiency, senescence, tyloses, vascular disease, *Vitis vinifera* L.

Introduction

The enormous anatomical diversity of flowering plants is a visual representation of their evolution and adaptation to different living environments (Crang et al. 2018). Plants can modify the anatomy of their cells, tissues and organs based on different environmental conditions and in response to abiotic and biotic stresses (Bortolami et al. 2019, Trueba et al. 2022). Xylem

vascular occlusions are considered a functional anatomical trait that result in response to a broad range of environmental and biotic factors (De Micco et al. 2016). They can be caused by gels (or gums), formed by amorphous extracellular materials (Rioux et al. 1998) and tyloses, which are expansions of parenchyma cells inside the vessel lumen (Zimmermann, 1979). Vascular occlusions have been identified during the senescence

process induced by different causes, such as tissue aging (Dute et al. 1999, Salleo et al. 2002), wounding (Sun et al. 2007, 2008), flooding (Davison and Tay, 1985) and vascular diseases (Pouzoulet et al. 2019, Mensah et al. 2020). In general, vascular occlusions are formed to hydraulically isolate specific regions of the plant, contributing to wound or pathogen compartmentalization (Pearce, 1996) and increasing decay resistance and mechanical support during heartwood formation (De Micco et al. 2016). The consequences of these occlusions have been largely studied in woody perennial organs, where they are thought to contribute to plant resistance to vascular pathogens (Park and Juzwik, 2014, Venturas et al. 2014, Rioux et al. 2018). However, they sometimes can lead to decreased hydraulic conductivity (McElrone et al. 2010, Deyett et al. 2019, Mensah et al. 2020, Fanton et al. 2022), and many theoretical articles have hypothesized that excessive production of vascular occlusions during disease could lead to lethal impairment in plant water transport (Fradin and Thomma, 2006, Yadeta and Thomma, 2013, Oliva et al. 2014).

In leaves, xylem occlusions have been studied during natural autumn senescence (Salleo et al. 2002) and induced premature senescence by the bacterium *Xylella* spp. (Fritschi et al. 2008, Choat et al. 2009), but their functions or effects on leaf physiology are still unknown. In addition, published reviews on leaf senescence (defined here as the degradation of the cellular structures and transition in cellular metabolism, Woo et al. 2013) have focused on molecular mechanisms, rather than the anatomical and physiological changes that occur in the xylem (Lim et al. 2007, Schippers et al. 2015), probably because vascular occlusions are frequently observed at the late stages of the senescence process (Chaffey and Pearson, 1985). In this context, exploring the underlying origins of xylem occlusions and their effects on plant physiology may improve our understanding of their functional role in leaf senescence resulting from different environmental factors.

Recently, we have associated vascular occlusions with *in vivo* quantification of xylem hydraulic failure in midribs, petioles and stems during the development of leaf symptoms caused by the grapevine trunk disease esca (Bortolami et al. 2019, 2021a). The wood-infecting fungal pathogens damage the host's vascular system, through enzymatic decomposition of woody cells/tissues and/or production of phytotoxin metabolites (Lecomte et al. 2012, Gramaje et al. 2018). Strikingly, vascular occlusions in esca symptomatic leaves or stems were observed at a distance from pathogen infection localized in the trunk or wounds (Bortolami et al. 2019, 2021a). This fatal disease impacts grape yield and quality worldwide (Mondello et al. 2018), and while its severity appears to have a relationship with climate (Bortolami et al. 2021b), the mechanisms behind leaf (and plant) death are largely unknown (Claverie et al. 2020).

In grapevine, premature or age-dependent leaf senescence induced by different stressors leads to similar physiological

responses and leaf symptom phenotypes that are sometimes hard to distinguish. Esca leaf symptoms consist of partial and total leaf discoloration and scorching, followed by leaf fall (Calzarano et al. 2014), similar to some mineral deficiencies and naturally occurring autumn senescence. Moreover, a decrease in stomatal conductance was observed during autumn senescence (Douthe et al. 2018, Gowdy et al. 2022), premature senescence induced by magnesium deficiency (Rogiers et al. 2020) and esca (Bortolami et al. 2021b). Therefore, we hypothesized that grapevine leaves affected by different stresses would be associated with similar responses of xylem anatomy, namely, the presence of vascular occlusions. In this study, we compared midrib vascular occlusions during leaf symptom development from esca versus leaf senescence induced by magnesium deficiency and autumn in grapevine (*Vitis vinifera* L.). In addition, we focused on esca leaf symptoms, comparing occlusion production in leaves from esca-infected vineyards across different climatic regions and cultivars. Finally, we followed the progression of vascular occlusions during esca symptom development and, through the use of non-invasive visualization of embolism, we quantified the xylem hydraulic integrity in the blade.

Materials and methods

Plant material and symptoms of senescence

To quantify xylem occlusions during different senescence types, we sampled leaves from *V. vinifera* cultivars (cv) in the Vitadapt experimental plot (Van Leeuwen et al. 2019). This plot includes 52 cultivars grafted onto the Selection Oppenheim 4 (SO4) rootstock and planted in 2009 in the Bordeaux region (France, 44°47'23.8"N 0°34'39.7"W). As presented in Table 1, in August 2018, we sampled 17 healthy (control) leaves, 22 esca symptomatic leaves and 6 magnesium-deficient leaves from 5 grapevine varieties. In October 2018, we sampled from the same varieties 21 leaves with phenotypes of autumn senescence (Table 1). Examples of the sampled induced senescence leaf symptoms are presented in Figure S1 available as Supplementary data at *Tree Physiology* Online for a white (Chenin) and a red (Castets) cultivar. Single leaves presented partial or total discoloration, or scorched tissue in between the major veins, and we were able to distinguish the different stresses by the whole-plant symptom pattern. Esca leaf symptoms were identified by the so-called 'tiger-stripe' leaves, as described in Lecomte et al. (2012), in the entire length of the stems. We identified the magnesium-deficiency phenotype in plants with leaves with discolorations only located in the lower part of the canopy and with no scorching. We identified autumn senescence in leaves with total or partial discoloration at the end of the growing season.

To further explore leaf xylem anatomy during esca symptom development, symptomatic and healthy (control) leaves

Table 1. Sample size for vessel occlusion quantification in *V. vinifera* leaves collected in four different countries, eight varieties and different senescence types.

Region	Plantation year	Control asymptomatic	Esca symptomatic	Magnesium deficient	Autumn
France	2009	Castets <i>n</i> = 5	Castets <i>n</i> = 5	Castets <i>n</i> = 2	Castets <i>n</i> = 5
		Chenin <i>n</i> = 2	Chenin <i>n</i> = 5	Chenin <i>n</i> = 2	Chenin <i>n</i> = 3
		Mourvedre <i>n</i> = 3	Mourvedre <i>n</i> = 2	Mourvedre <i>n</i> = 2	Mourvedre <i>n</i> = 7
		Sangiovese <i>n</i> = 4	Sangiovese <i>n</i> = 5		Sangiovese <i>n</i> = 1
		Sauvignon blanc <i>n</i> = 3	Sauvignon blanc <i>n</i> = 5		Sauvignon blanc <i>n</i> = 5
Italy	1989	Sangiovese <i>n</i> = 3	Sangiovese <i>n</i> = 5	–	–
		Sauvignon blanc <i>n</i> = 3	Sauvignon blanc <i>n</i> = 4		
		Castets <i>n</i> = 3	Castets <i>n</i> = 5	–	–
Spain	2013	Tempranillo <i>n</i> = 3	Tempranillo <i>n</i> = 5		
		Tempranillo blanco <i>n</i> = 1	Tempranillo blanco <i>n</i> = 3		
		Grenache <i>n</i> = 1	Grenache <i>n</i> = 5		
		Sauvignon blanc <i>n</i> = 8	Sauvignon blanc <i>n</i> = 7	–	–
California (USA)	2000				

were sampled from eight cultivars (Castets, Chenin, Grenache, Mourvedre, Sangiovese, Sauvignon blanc, Tempranillo and Tempranillo blanco) from different countries (France, Italy, Spain and California in the USA). The exact number of replicates per country and variety is presented in Table 1. In France, we sampled 39 leaves from five cultivars of the Vitadapt plot in August 2018 as described above. In Italy (Carassai, Ascoli Piceno Province, 43°02'18.07"N 13°39'39.41"E), leaves were sampled in June 2019 from two *V. vinifera* cultivars, planted in 1989, grafted onto Kober 5BB rootstock. In Spain (La Rioja region, 42°26'19.7"N 1°49'30.5"W), leaves were sampled in late August 2019 from three *V. vinifera* cultivars, planted in 2013, grafted onto the 110 Richter (110R) rootstock. In California (in the North Coast regions, 39°00'15.1"N 122°51'08.3"W), leaves were sampled in August 2020 from one *V. vinifera* cultivar, planted in 2000, grafted onto the Teleki 5C (5C) rootstock.

To explore the evolution of occlusion formation over time during esca symptom development, we monitored esca leaf symptoms and sampled leaves on eight potted plants from June (day of the year, doy = 172) to September 2018 (doy = 262). The experimental setup is described in Bortolami et al. (2019). Briefly, 30-year-old *V. vinifera* cv Sauvignon blanc vines, grafted onto the Millardet de Grasset 101–14 (101–14 MGt) rootstock, were uprooted from the field in February 2018 and transferred into 20 l pots. We sampled, over the experimental season 2018, 45 leaves from 3 control asymptomatic plants and 5 esca symptomatic plants. Leaf sample size was as follows: 8 control, 13 asymptomatic leaves before the plant expressed esca symptoms, 9 asymptomatic leaves from plants with symptomatic leaves and 15 esca symptomatic leaves. In September 2017 and 2018, we brought control and symptomatic plants to synchrotron SOLEIL (PSICHE beamline) and scanned leaf midribs with X-ray microCT, as described in Bortolami et al. (2019). The same midribs analyzed in Bortolami et al. (2019) are reported on here, but we report only novel data on the

percentage of occluded vessels quantification (in number), and not the theoretical loss of hydraulic conductivity (PLC).

Light microscopy and occlusion quantification

On each leaf, a 1-cm section of midrib was cut at 1 cm from the petiole point. Samples collected in France were directly put in an FAA solution composed of 0.64% paraformaldehyde, 50% ethanol, 5% acetic acid and 44.36% water (v/v). After 1 to 3 days in the FAA solution on a shaker at 90 r.p.m., samples were dehydrated using a graded series of alcohol (80, 100 and 100% for 30 min each) and stored at 4 °C until analysis. Samples collected in California, Italy and Spain were put directly in 80% alcohol, mailed to France and stored at 4 °C until analysis. After one night in the FAA solution, samples were dehydrated using the same graded series (80, 100 and 100% v/v for 30 min each). Samples were then embedded using a graded series of LR White resin (Agar scientific Ltd., Essex, U.K., 33, 50 and 66% LR White v/v in ethanol solution for 120 min each, and 100% three for 7 h each). Finally, samples were polymerized in capsules at 60 °C for 24–48 h. Transverse sections of 1.8 to 2 µm thickness were cut using an Ultracut S microtome (Reichert, Leica, Vienna, Austria) equipped with a glass knife at the Bordeaux Imaging Center, a member of the France Bio Imaging national infrastructure (ANR-10-INBS-04). Cross sections were stained with 0.05% (w/v) Toluidine Blue O. Stained sections were dried and photographed with a DS-Fi3 camera (Nikon, France) mounted on a stereo microscope SMZ1270 (Nikon). By the use of Toluidine blue O dye, we identified the nature of vascular occlusions, which includes gels (i.e. amorphous extracellular material, mainly composed by pectins and polysaccharides, Figure 1B and D) and tyloses (i.e. expansions of the neighbor-vessels parenchyma cells, Figure 1B and D).

Xylem vessels were identified and quantified in one entire cross-section per leaf using ImageJ (Schneider et al. 2012) and

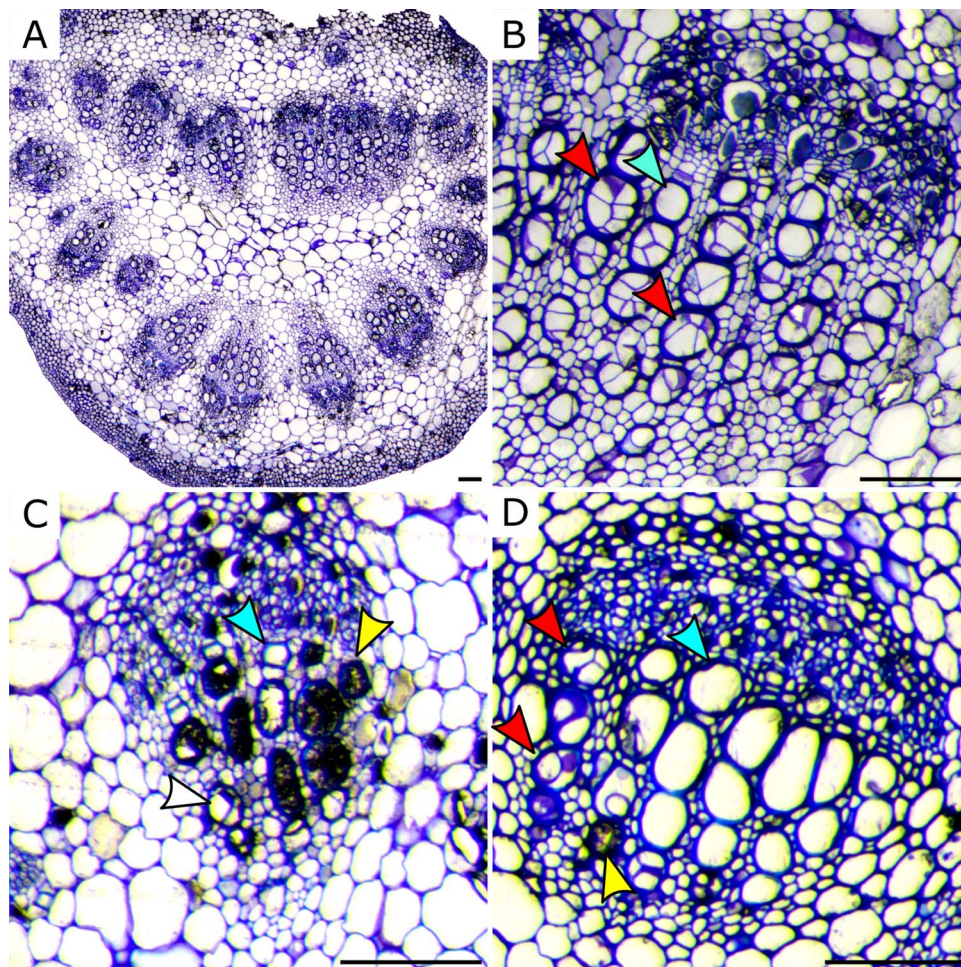


Figure 1. Xylem vessel anatomy in *V. vinifera* midribs. In whole midrib transverse cross-sections (A), vessels were classified according to: the absence of any structure in their lumina (i.e. apparently functional vessels; blue arrowheads, B–D); the presence of crystal depositions when druse crystals were covering the vessel surface (yellow arrowheads, C, D) or when prismatic crystals were identified (white arrowhead, B); the presence of occlusion when gel pockets and/or tyloses were observed in their lumina (red arrowhead, B, D). Scale bars = 100 μm .

categorized as empty vessels or occluded vessels (presenting gel or tyloses). In addition, we observed a deposition of crystals in vessels of 93% of the samples and thus quantified their presence. To confirm that vascular occlusions were equally distributed within a sample (i.e. in the 1-cm segment), we quantified vascular occlusions in three cross-sections along the segment (i.e. subsamples) for 29 (over the 177 analyzed) midribs. We found that the presence of occlusions did not significantly differ among cross sections within a sample ($F_{55,12,498} = 0.97$, $P = 0.54$, treating repetition, sample identity and their interaction as fixed effects in an independent linear model, with a binomial distribution for presence/absence of an occlusion, in SAS using the GLIMMIX procedure).

Non-invasive optical determination of xylem functionality

To investigate the extent to which esca impacts xylem functionality and leaf embolism resistance, the onset and propagation of embolism were evaluated in 4 leaves from 3 different

control asymptomatic plants and in 11 leaves from 4 different esca symptomatic plants, using the optical vulnerability (OV) technique (Brodrigg et al. 2016) during a dry-down experiment. In every leaf, the region of interest (i.e. the scanned area) included the midrib (at 3–5 cm from the apex of the leaf) in the middle of the scan and approximately 10×3 cm around it. The experiment took place over 2 weeks (in September 2019) on >2 -m long stems of potted *V. vinifera* cv Sauvignon blanc plants uprooted in February 2019 from the same plot as the one used for the leaf midrib sampling for occlusion quantification (INRAE, Bordeaux). In the early morning, stems were cut under water at their base, put inside dark plastic bags with humid paper and rapidly transported to the lab. Once at the lab, the abaxial side of intact leaves was fixed on a scanner (Perfection V800 Photo, EPSON, Suna, Japan) using a transparent glass and adhesive tape. Brightness and contrast as well as leaf scanned area were adjusted to optimize visualization of embolisms. Imaging of 991 ± 90 mm² (average \pm SE) of each leaf was automatically

performed every 5 min throughout plant dehydration using a computer automation software (Autolt 3). Upon completion, the stacks of images, consisting of 1800 to 2000 scans per leaf, were analyzed to highlight embolism events revealed as changes in light transmission through the leaf xylem. Analyses were carried out using ImageJ software and following instructions from <http://www.opensourceov.org>. Briefly, total embolism was quantified by subtracting pixel differences between consecutive images (i.e. pixel values that did not change resulted in a value of zero). In these series, white pixels represented leaf embolism. Noise was removed using the ImageJ outlier removal, and pixel threshold was used to extract embolism from any background noise remaining. The embolism area per image was calculated as the sum of non-zero pixels on the total scanned surface (mm²) or on green leaf surface only (mm², excluding the symptomatic tissue). We considered the veins that embolized as functional (i.e. containing water under tension), while the remaining veins were considered as non-functional (i.e. containing any combination of air, occlusion or static water). As stems dehydrated, stem water potential (Ψ_{stem}) was simultaneously monitored every 30 min using psychrometers (ICT Internationale, Armidale, NSW, Australia), which were installed in the middle of the stem prior to the start of the experiment (i.e. when stems were fully hydrated). The accuracy of psychrometer readings was assessed periodically with a Scholander pressure bomb (SAM Precis, Gradignan, France), using leaves adjacent to the scanned ones and that had been covered for at least 2 h with aluminum foil and wrapped in a plastic bag.

Esca leaf symptom severity

Each leaf was photographed before sampling for the leaf xylem anatomy and OV measurements during esca symptom development. We quantified the percentage of green tissue on the upper face of each leaf using ImageJ in order to estimate leaf esca symptom severity. On samples used for OV measurements, this estimation was done on the scanned area only, not on the whole leaf surface. We first detected the green hue ranges on RGB pictures of control-asymptomatic leaves using the color threshold in ImageJ, and then used these green ranges to select and quantify the green pixels in each photo. We finally reported these values to the total leaf surface and obtained a percentage of green tissue per leaf or area analyzed. In every cultivar, we covered the esca symptom severity spectrum (from low to high percentage of green tissue) as much as possible in order to avoid sampling bias.

Statistical analysis

We investigated whether induced senescence types and cultivars are associated with the probability of occlusion formation in xylem vessels using multiple generalized linear mixed models to compare control versus esca symptomatic plants (fixed effect). Prior to analysis, the data (bounded

between 0.0001 and 1) were transformed using a logit function as appropriate for analyzing proportions (Warton and Hui, 2011). In order to use the logit function the lowest value of 0.0001 was assigned to samples with no presence of occlusions. We investigated whether esca symptomatic and control leaves presented different response in embolized surface during decreasing Ψ_{Stem} using a generalized linear mixed model with the plant treated as random effect and the interaction between symptom presence and Ψ_{Stem} as a fixed effect. The relationships between the percentage of occluded vessels and esca symptom severity (expressed in percentage of leaf green tissue) were tested using linear regression models. The effect of the age of symptom on the amount of vascular occlusion was tested with a general linear mixed model on symptomatic leaves, using the sampling date as fixed effect and the plant as random effect. All statistical tests were performed using the SAS software (SAS 9.4; SAS Institute). We used the GLIMMIX procedure for generalized linear mixed models, and the REG procedure for regression analyses. The normality of the response variables was tested using a Kolmogorov–Smirnov test implemented in the UNIVARIATE procedure, prior to analyses.

Results

Anatomical diversity of vascular occlusions and presence of crystals

In each sample, we categorized the vessels as occluded by gels and/or tyloses, with depositions of crystals, or with an absence of any structure (Figure 1). Crystals (both druse and prismatic) were present inside some vessel lumen (in 15% of vessels on average, Figure 1C). These crystals were more often present in samples from which occlusions were absent (on average, 21% of vessels with crystals in control leaves, versus 10% in esca symptomatic leaves, Figure S2 available as Supplementary data at *Tree Physiology Online*). We showed that control (asymptomatic) leaves (almost) never had occlusions (in 2% of vessels on average, Figures 2–4), and that under microCT X-ray scans (data from Bortolami et al. 2019) and optical visualizations (Figure 5) they were almost fully functional. This relationship suggests that crystals are likely present in functional rather than occluded vessels (see Supplemental discussion SD1 available as Supplementary data at *Tree Physiology Online* for details). Consequently, to evaluate the impact of different stresses on xylem anatomy and water transport, we reported here only the percentages of occlusions, and not of crystals, in different experiments and comparisons.

Vascular occlusions in senescing leaves

To investigate the presence of occlusion during the autumnal or premature leaf senescence induced by different causes, we compared midribs from control, esca symptomatic, magnesium deficient and autumn senescent leaves (Figure 2). The amount

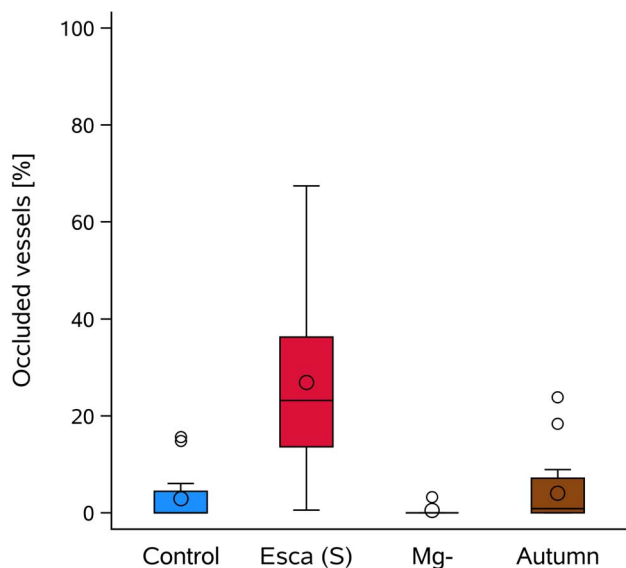


Figure 2. Percentage of occluded vessels in *V. vinifera* midribs of control leaves and leaves from three types of leaf symptom (esca leaf symptoms, magnesium deficiency, autumn senescence). Colors correspond to midribs from: healthy leaves (control) (blue, $n = 17$), esca symptomatic (red, $n = 22$), magnesium deficiency (gray, $n = 6$) and autumn senescence (brown, $n = 21$) leaves. Boxes and bars show the median, quartiles and extreme values. Larger circles within boxes correspond to means and smaller circles outside boxes to outlier values.

of vessel occlusions in midribs significantly differs among the four leaf categories ($F_{3,62} = 19.4$, $P < 0.0001$). Midribs in esca-symptomatic leaves presented the highest percentage of occluded vessels ($27\% \pm 4$, average \pm SE) compared with autumn-senescent leaves ($4.0 \pm 1\%$), control leaves ($2.9 \pm 1\%$) and magnesium-deficient leaves, which had the lowest percentage of occluded vessels ($0.53 \pm 0.5\%$). However, two autumn-senescent midribs, which were statistical outliers, had over 15% occluded vessels (Figure 2).

Vascular occlusions in esca symptomatic leaves from different cultivars and countries

We quantified the percentage of occluded vessels in esca symptomatic and control (asymptomatic) leaf midribs from four different countries (France, Italy, California in the USA and Spain) in eight cultivars: Castets, Chenin, Grenache, Mourvedre, Sangiovese, Sauvignon blanc, Tempranillo and Tempranillo blanco (Figure 3, Figure S3 and Table S1 available as Supplementary data at *Tree Physiology* Online). Our results show that esca symptomatic leaves presented a significantly higher presence of occlusions compared with controls ($F_{1,93} = 85.93$, $P < 0.0001$), see Table S1 available as Supplementary data at *Tree Physiology* Online for the detailed comparisons within varieties and countries. Cultivars had significantly different levels of occlusions among the symptomatic samples ($F_{7,48} = 13.55$, $P < 0.0001$ Figure 3A). However, the variability was high,

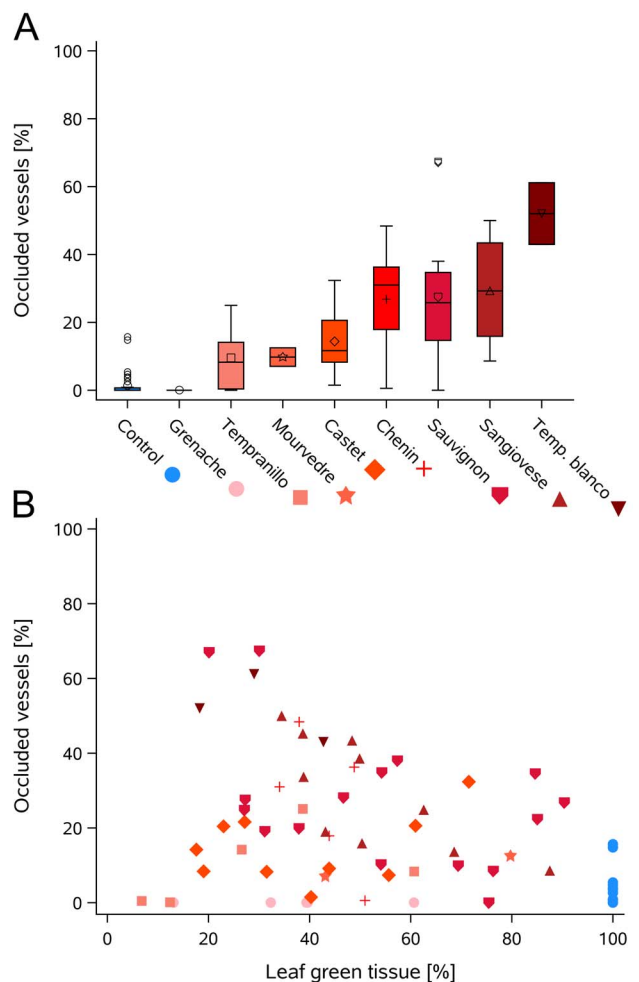


Figure 3. Occluded vessels (%) in different cultivars from different countries in *V. vinifera* midribs of leaves with (red shades) or without (blue) esca leaf symptoms. (A) Percentage of occluded vessels in midribs from control leaves (blue, all control leaves from all cultivars and countries combined) and esca symptomatic (from light red to dark red, all countries combined) leaves. Boxes and bars show the median, quartiles and extreme values. Larger symbols within boxes correspond to means and smaller symbols outside boxes to outlier values. The statistical differences are presented in the text. An additional analysis between each cultivar and its specific control per country is presented in Table S1 available as Supplementary data at *Tree Physiology* Online. (B) Relationship between the percentage of occluded vessels and esca symptom severity (expressed in percentage of green tissue per leaf). Control leaves were excluded from the statistical analysis but are represented on the graphics as blue filled circles for illustration. The colors and markers are the same as panel A: circles for Grenache, squares for Tempranillo, stars for Mourvedre, diamonds for Castets, plus for Chenin, pentagons for Sauvignon blanc, upside-triangles for Sangiovese and downside-triangles for Tempranillo blanco. The regressions for each cultivar are presented in Table S2 available as Supplementary data at *Tree Physiology* Online, where a significant relationship was found only for Sangiovese.

ranging from no occlusion in symptomatic Grenache midribs to $52 \pm 5\%$ of occluded vessels in symptomatic Tempranillo blanco midribs (Figure 3A). Leaf symptom severity (quantified as the percentage of green leaf tissue) had no significant effect

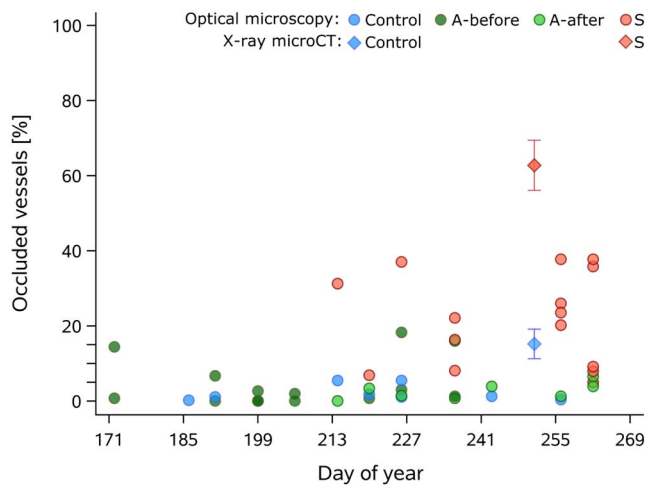


Figure 4. Evolution of occluded vessels (%) over the season (July to September) in *V. vinifera* cv Sauvignon blanc midribs. Symbols correspond to single leaves from well-watered control plants (blue, $n = 8$), asymptomatic leaves before esca symptom appearance (dark green, $n = 13$), asymptomatic leaves (light green, $n = 9$) and esca symptomatic (red, $n = 15$) leaves from plants with symptomatic leaves. Circles correspond to optical microscopy observations; diamonds correspond to X-ray microCT scan analyses (data from Bortolami et al. 2019). In X-ray microCT quantification, symbols correspond to means and bars to \pm SE ($n = 8$ control in blue and $n = 13$ esca leaves in red).

on the leaf occlusion level within symptomatic leaves, except for Sangiovese (Figure 3B, Table S2 available as Supplementary data at *Tree Physiology* Online). Nevertheless, the most occluded leaves (above 40%) had the most severe symptoms (less than 40% of green tissue), and among the mildly symptomatic leaves (more than 60% of green tissue) the occlusions rarely occupied more than 30% of the vessels (Figure 3B). When considering the control leaves (entirely green) in the statistical analysis, the percentage of occluded vessels was significantly related to the percentage of leaf green tissue ($R^2 = 0.31$, $P < 0.0001$).

Vascular occlusion evolution during esca symptom appearance

During one experimental season, we monitored esca leaf symptoms on eight potted plants from June (doy = 172) to September 2018 (doy = 262, Figure 4). The symptoms developed at the same time in the season; hence, using 'doy' as a good comparison to evaluate the effect of symptom age on occlusion formation. Using light microscopy, we found that control plants always had low levels of occlusions inside their midribs, as was the case for the majority of asymptomatic leaves both before and after symptoms appeared on other leaves on the same plant (<7% of occluded vessels, Figure 4). Ten out of 15 symptomatic leaves had a higher level of occlusions (>14%) compared with controls, as well as 2 leaves before symptom appearance, and 1 asymptomatic leaf from a symptomatic plant (Figure 4). Overall, we found a significant effect of the presence

of esca symptoms on the amount of vessel occlusions (i.e. comparing the four leaf categories in Figure 4, $F_{3,35} = 9.36$, $P = 0.0001$), but there were no changes in the occlusion level over time within the symptomatic leaves ($F_{5,5} = 1.19$, $P = 0.43$), suggesting that occlusions do not increase with symptom age. Scanning midribs with X-ray microCT, we found higher average occluded vessels (compared to light microscopy) both in control and symptomatic midribs (15.2 ± 4 and $62.7 \pm 7\%$, average \pm SE, respectively, Figure 4).

The hydraulic consequences of xylem occlusions

Using a non-invasive optical vulnerability technique, we were able to quantify the embolism spread in control and esca symptomatic leaf veins (Figures 5 and 6). At the end of dehydration, when no supplemental embolism formation was detected, we summed all the embolism events within a sample (red vessels, Figure 5). We found that almost all the veins embolized in control leaves (Figure 5A–D), whereas the veins did not embolize in wide portions of the leaf blade in esca symptomatic leaves (Figure 5E–M), especially in between the main veins where the leaf was yellow and scorched. In two symptomatic leaves no embolism event was observed (Figure 5N, O). In most symptomatic leaves, the primary and secondary order veins readily embolized, whereas the tertiary or above order veins did not. Plotting the embolism spread versus the decrease in stem water potential, we found that control leaves had a final embolized area of $25.1 \pm 7 \times 100$ pixels mm^{-2} on the entire scanned area, compared with $5.2 \pm 2 \times 100$ pixels mm^{-2} in symptomatic leaves (Figure 6A). When only the green surface of the leaves was considered (i.e. excluding the symptomatic discolored and scorched tissues; Figure 6B), control leaves had the same embolized area evolution (they were completely green), whereas symptomatic leaves had a final embolized area of $13.0 \pm 4 \times 100$ pixels mm^{-2} (Figure 6B). We found a significant effect of esca both considering the whole scanned surface ($F_{2,456} = 219.05$ $P < 0.0001$) or only the green area ($F_{2,456} = 128.80$ $P < 0.0001$). In control leaves, embolism events were detected between -1.9 and -3.3 MPa (Figure 6A and B), whereas in symptomatic leaves these events appeared across a larger range of Ψ_{stem} (i.e. between -1.3 and -4.9 MPa, Figure 6A and B). Finally, it is worth noting that the total embolized area of symptomatic leaves was almost always less ($21 \pm 0.1\%$) than half that of the control leaves (noted with the horizontal line in Figure 6B).

Discussion

In this study, we highlight the uniqueness of esca leaf symptoms compared with other induced senescence processes. We demonstrated that only esca symptomatic leaves had significant levels of occluded vessels in their midribs compared to those of leaves with magnesium deficiency or undergoing autumn

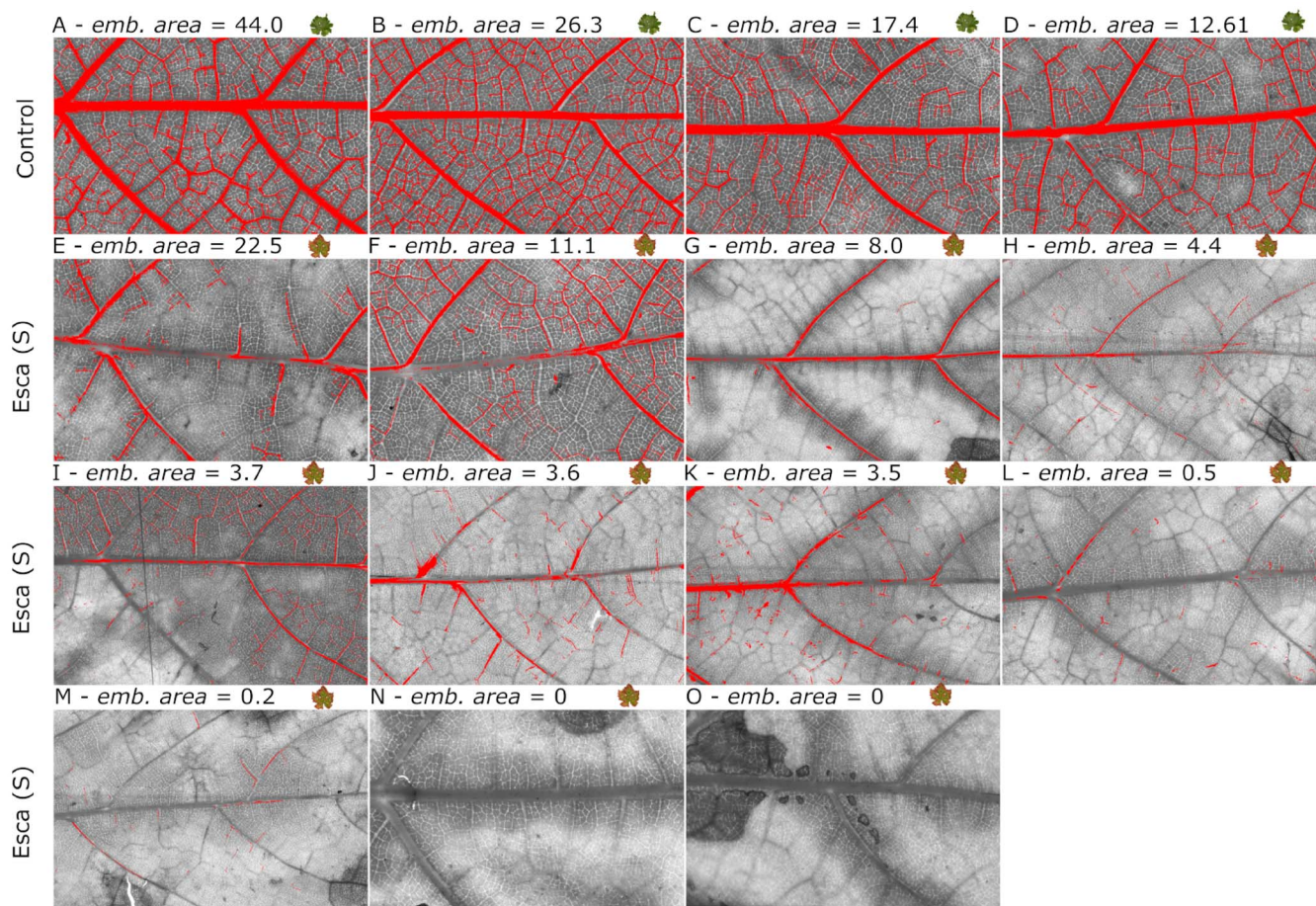


Figure 5. Visualization of embolism formation during dehydration of *V. vinifera* cv Sauvignon blanc leaves from control and esca symptomatic leaves. Each panel corresponds to a leaf blade from control leaves collected on asymptomatic control plants (A–D) and esca symptomatic leaves (E–O). Red veins correspond to veins that embolized at the end of dehydration. The total cumulative embolized area (emb. area) is indicated for each sample ($\times 100$ pixels mm^{-2}).

senescence. We investigated esca leaf symptoms in detail and demonstrated that the percentage of occlusion: (i) varied among cultivars and (ii) were similar among symptomatic leaves collected throughout the season (i.e. occlusions did not increase over time). Finally, using the optical vulnerability (OV) technique, we explored the hydraulic integrity in esca symptomatic leaves. Our finding of non-functional vessels across large portions of esca symptomatic leaf blade, compared with the highest density of functional xylem vessels in the midrib, suggests that vascular occlusions are localized near the scorched and discolored areas of the leaves in between the major veins and at the margins of the leaf.

Esca, a unique senescence process

Comparing different leaves with different senescence types, esca leaf symptoms had the highest levels of vessel occlusion. Both magnesium deficiency and autumn senescence types share in common with esca a leaf chlorosis and a decrease in stomatal conductance (Salleo et al. 2002, Brodribb and Holbrook, 2003 for autumn senescence, Tränkner et al. 2016, Rogiers et al.

2020 for magnesium deficiency and Lecomte et al. 2012, Bortolami et al. 2021b for esca). Given that occlusions were absent from leaves with magnesium deficiency, it is likely that the impacts of magnesium deficiency on leaf gas exchange are not related to a loss of leaf xylem hydraulic conductivity. During autumn senescence, occlusions have been detected in parts of the leaf we did not examine, namely the petioles and the stem-petiole junction (Chattaway, 1949, Salleo et al. 2002, De Micco et al. 2016). Indeed, during autumn, the hydraulic conductivity decreases in petioles, but not in leaf blades (Salleo et al. 2002). This difference in the spatial distribution of occlusions suggests that the visible similarities between esca symptom leaves and autumn senescence (described above) are due to different mechanisms. In the most prominent hypothesis of esca leaf symptom formation, toxins are translocated from the fungal biomass (the pathogens reside in the woody tissues) out to the leaves through the vascular system (Claverie et al. 2020). Previously, using microCT X-ray, we showed that more basal organs (stems, Bortolami et al. 2021a) are less occluded than distal organs (petioles and midribs, Bortolami et al. 2019). Here,

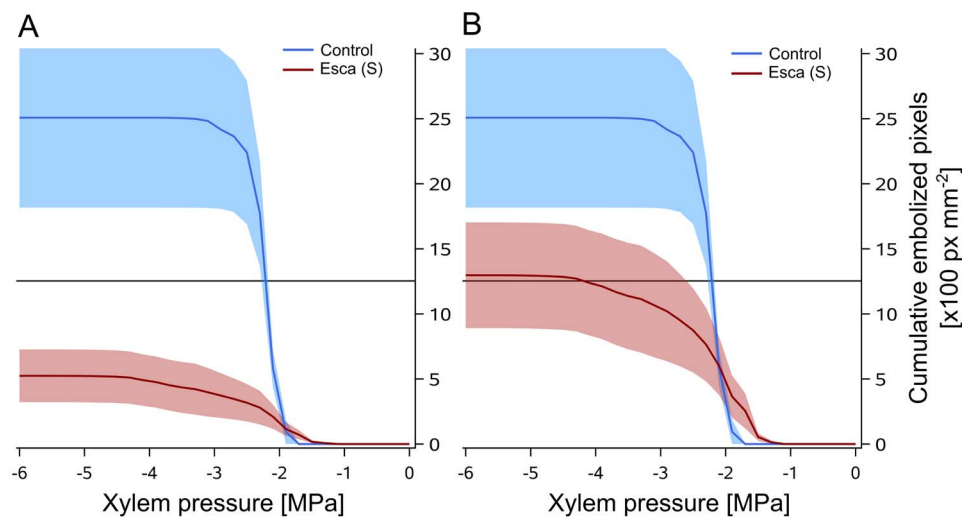


Figure 6. Embolism formation in leaf blade from *V. vinifera* cv Sauvignon blanc from control (blue) and esca symptomatic (red) leaves during dehydration. (A) Sum of embolized pixels on the total (green and symptomatic) scanned surface over decreasing xylem pressure. (B) Sum of embolized pixels on the green scanned area (i.e. excluding symptomatic discolored portions) over decreasing xylem pressure. Lines (moving averages over 0.2 MPa) represent the average evolution of embolized areas ($\times 100$ pixels mm^{-2}) during decreasing xylem pressure (MPa). The bands represent the SE for each group, and the horizontal black lines correspond to 50% of embolized area for control leaves.

we show that occlusions are more frequent in the leaf blade than in the midribs (Figure 5), supporting the hypothesis that fungal toxins are expected to accumulate, and thus initiate a host response in the form of xylem occlusions, where the water flow ends (i.e. peripheral veins). In contrast, during autumn senescence the hormones that initiate the senescence process are synthesized in situ (Schippers et al. 2015), suggesting a more local response in the vasculature (for example, only at the abscission point in petioles).

Exploring the vascular occlusions and hydraulic integrity during esca leaf symptoms

Comparing esca symptomatic leaves among cultivars and countries, we found significant levels of occlusion in the majority of the symptomatic leaves analyzed. It has been previously demonstrated that Sauvignon blanc vines (30-year-old plants transplanted from the vineyard into pots and grown in a greenhouse) suffer from occlusion-driven hydraulic failure during esca leaf symptom expression (Bortolami et al. 2019, 2021a). Here, we demonstrated that occlusions (and subsequent hydraulic failure) are also associated with esca in the field, and this finding is not particular to one specific climate or cultivar (or to our previous greenhouse experiment). However, the range of occlusion levels among cultivars is noteworthy and suggests differences between genotypes regarding the extent of vascular occlusion. This is consistent with the fact that, during other vascular diseases, occlusions can be considered beneficial up until the point at which they impact plant function. In the first case, occlusions efficiently compartmentalize pathogens and limit the spread of infection within a plant (Clérvet et al. 2000, Rioux et al. 2018, Pouzoulet et al. 2020); in the second case,

occlusions interfere with water movement, generating hydraulic failure with detrimental consequences for the plant (Sun et al. 2013, Mensah et al. 2020). When a xylem vessel is occluded, we cannot separate these two consequences. Especially in the case of esca, where the subsequent reduction in water flow should reduce the spread of pathogen-derived toxins as well, while suppressing xylem functionality by hydraulic failure. More studies are needed to test this hypothesis and relate vascular occlusion rates to plant mortality relative to the degree of esca susceptibility in each cultivar.

Following occlusions in leaves from symptomatic plants throughout the season, we observed that esca symptomatic leaves had a higher proportion of occluded vessels than asymptomatic leaves from the same plants and healthy leaves from control plants. Moreover, levels of occlusions were similar throughout the season, indicating that the number of occlusions does not increase over time, but is coincident with the onset of symptoms. In 3 out of 22 samples, occlusions were present in asymptomatic leaves from plants with other symptomatic leaves (light and dark green dots above 10% in Figure 4). At the same time, we also observed that visual symptoms were sometimes (in 5 out of 15 samples) associated with low levels of occlusions (red dots in Figure 4). These results are also consistent with the comparison among and within cultivars, where the level of occlusions was not related to symptom severity (Figure 3B). We could explain this variability by the fact that we analyzed 2- μm -thick cross-sections on midribs, which can reach 20 cm in length, and as such, we may have underestimated occlusions. Indeed, if we quantified more non-functional vessels using microCT X-ray it is also because we could explore 1 cm volume in each sample, increasing the

probability of observing occlusions. The comparison with the optical embolism visualization supports this hypothesis, as the midribs are not uniformly functional (or non-functional) along their length. From optical visualizations, we considered each vein with an embolism event during dehydration (i.e. containing water under tension) as functional. We observed that midribs are the most functional parts in symptomatic leaves (Figure 5) and that many regions of leaf blade were already non-functional before we started the dry-down experiment. We can conclude that occlusion-driven hydraulic failure may have a stronger impact on the total leaf hydraulic conductivity than what was previously estimated by X-ray scans in midribs (Bortolami et al. 2019). Moreover, even when only the remaining green asymptomatic part of the leaves was considered, we quantified that the relative embolized surface was lower in symptomatic leaves compared with controls, reinforcing the hypothesis that vascular occlusions strongly affect the leaf xylem functionality of grapevines with esca.

Conclusions

In this study, we showed that esca leaf symptoms are associated with anatomical modifications that are unique to its proper premature leaf senescence process. Indeed, no vascular occlusions were detected in leaves with magnesium deficiency or autumn senescence. This result reinforced the particularity of esca over other induced senescence types, highlighting the need to understand the underlying physiological (and pathological) mechanisms of esca pathogenesis. Importantly, this work confirms that vascular occlusions in leaves during esca are associated with hydraulic failure in the leaf blade. The different cultivar (and climatic) susceptibility in occlusion formation during esca could also open new perspectives regarding the use of occlusion quantification to characterize plant resistance to the disease.

Data and Materials Availability

Data and materials are available to academic researchers on reasonable request.

Supplementary data

Supplementary data for this article are available at *Tree Physiology* Online.

Acknowledgments

We thank Mark Gowdy and Agnès Destrac-Irvine from UMR EGFV (INRAE) for providing technical help in the Vitadapt plot. We thank the team of UMR SAVE (INRAE) for the technical support in the greenhouse experimentations. We thank Patrick Leger and Régis Burlett from UMR BIOGECO (INRAE) for help with the optical vulnerability method implementation and the SOLEIL

synchrotron facility (HRCT beamline PSICHE) for providing the materials and logistics.

Author's contributions

G.B., C.E.L.D. and G.A.G. designed the experiments; G.B., K.B., D.G. and G.R. conducted the leaf sampling; N.F. conducted the histological observations; L.J.L. and S.D. conducted the non-invasive optical visualization of embolism and analyzed the images; G.B. analyzed the images from light microscopy and analyzed the data; G.B., C.E.L.D. and G.A.G. wrote the article; all authors edited and agreed on the last version of the article.

Funding

This work was supported by the French Ministry of Agriculture, Agrifood and Forestry (FranceAgriMer and CNIV) within the PHYSIOPATH project (program Plan National Dépérissement du Vignoble, 22001150–1506) and the LabEx COTE (ANR-10-LABX-45) 'Projet Caviplace Platform'.

Conflict of interest

None declared.

References

- Bortolami G, Gambetta GA, Delzon S et al. (2019) Exploring the hydraulic failure hypothesis of esca leaf symptom formation. *Plant Physiol* 181:1163–1174.
- Bortolami G, Farolfi E, Badel E et al. (2021a) Seasonal and long-term consequences of esca grapevine disease on stem xylem integrity. *J Ex Bot* 72:3914–3928.
- Bortolami G, Gambetta GA, Cassan C, et al. (2021b) Grapevines under drought do not express esca leaf symptoms. *Proc Natl Acad Sci USA* 118:e2112825118. <https://doi.org/10.1073/pnas.2112825118>.
- Brodribb TJ, Holbrook NM (2003) Stomatal closure during leaf dehydration, correlation with other leaf physiological traits. *Plant Physiol* 132:2166–2173.
- Brodribb TJ, Skelton RP, McAdam SAM, Bienaimé D, Lucani CJ, Marmottant P (2016) Visual quantification of embolism reveals leaf vulnerability to hydraulic failure. *New Phytol* 209:1403–1409.
- Calzarano F, Di Marco S, D'Agostino V, Schiff S, Mugnai L (2014) Grapevine leaf stripe disease symptoms (esca complex) are reduced by a nutrient and seaweed mixture. *Phytopathol Mediterr* 53:543–558.
- Chaffey NJ, Pearson JA (1985) Presence of tyloses at the blade/sheath junction in senescing leaves of *Lolium temulentum* L. *Ann Bot* 56:761–770.
- Chattaway M (1949) The development of tyloses and secretion of gum in heartwood formation. *Aust J Biol Sci* 2:227–240.
- Choat B, Gambetta GA, Wada H, Shackel KA, Matthews MA (2009) The effects of Pierce's disease on leaf and petiole hydraulic conductance in *Vitis vinifera* cv. Chardonnay. *Physiol Plant* 136:384–394.
- Clavier M, Notaro M, Fontaine F, Wery J (2020) Current knowledge on Grapevine Trunk Diseases with complex etiology: a systemic approach. *Phytopathol Mediterr* 59:29–53.
- Clériveret A, Déon V, Alami I, Lopez F, Geiger J-P, Nicole M (2000) Tyloses and gels associated with cellulose accumulation in vessels

- are responses of plane tree seedlings (*Platanus × acerifolia*) to the vascular fungus *Ceratocystis fimbriata* f. sp. *platani*. *Trees* 15:25–31.
- Crang R, Lyons-Sobaski S, Wise R (2018) Plant anatomy: a concept-based approach to the structure of seed plants. Springer Nature Switzerland: Springer international publishing, <https://doi.org/10.1007/978-3-319-77315-5>.
- Davison EM, Tay FCS (1985) The effect of waterlogging on seedlings of *Eucalyptus marginata*. *New Phytol* 101:743–753.
- De Micco V, Balzano A, Wheeler EA, Baas P (2016) Tyloses and gums: a review of structure, function and occurrence of vessel occlusions. *IAWA J* 37:186–205.
- Deyett E, Pouzoulet J, Yang J-I, Ashworth VE, Castro C, Roper MC, Rolshausen PE (2019) Assessment of Pierce's disease susceptibility in *Vitis vinifera* cultivars with different pedigrees. *Plant Pathol* 68:1079–1087.
- Douthe C, Medrano H, Tortosa I, Escalona JM, Hernández-Montes E, Pou A (2018) Whole-plant water use in field grown grapevine: seasonal and environmental effects on water and carbon balance. *Front Plant Sci* 9:1540. <https://doi.org/10.3389/fpls.2018.01540>.
- Dute RR, Duncan KR, Duke B (1999) Tyloses in abscission scars of loblolly pine. *IAWA J* 20:69–74.
- Fanton AC, Furze ME, Brodersen CR (2022) Pathogen-induced hydraulic decline limits photosynthesis and starch storage in grapevines (*Vitis* sp.). *Plant Cell Environ* 45:1829–1842.
- Fradin EF, Thomma BPHJ (2006) Physiology and molecular aspects of Verticillium wilt diseases caused by *V. dahliae* and *V. albo-atrum*. *Mol Plant Pathol* 7:71–86.
- Fritschi FB, Lin H, Walker MA (2008) Scanning electron microscopy reveals different response pattern of four vitis genotypes to *Xylella fastidiosa* infection. *Plant Dis* 92:276–286.
- Gowdy M, Pieri P, Suter B, Marguerit E, Destrac-Irvine A, Gambetta GA, van Leeuwen C (2022) Estimating bulk stomatal conductance in grapevine canopies. *Front Plant Sci* 13. <https://doi.org/10.3389/fpls.2022.839378>.
- Gramaje D, Úrbez-Torres JR, Sosnowski MR (2018) Managing grapevine trunk diseases with respect to etiology and epidemiology: current strategies and future prospects. *Plant Dis* 102:12–39.
- Lecomte P, Darrieutort G, Liminana J-M, et al. (2012) New insights into esca of grapevine: the development of foliar symptoms and their association with xylem discoloration. *Plant Dis* 96:924–934.
- Lim PO, Kim HJ, Gil Nam H (2007) Leaf senescence. *Annu Rev Plant Biol* 58:115–136.
- McElrone AJ, Grant JA, Kluepfel DA (2010) The role of tyloses in crown hydraulic failure of mature walnut trees afflicted by apoplexy disorder. *Tree Physiol* 30:761–772.
- Mensah JK, Sayer MAS, Nadel RL, Matusick G, Eckhardt LG (2020) Physiological response of *Pinus taeda* L. trees to stem inoculation with *Leptographium terebrantis*. *Trees* 34:869–880.
- Mondello V, Songy A, Battiston E, Pinto C, Coppin C, Trotel-Aziz P, Clément C, Mugnai L, Fontaine L (2018) Grapevine trunk diseases: a review of fifteen years of trials for their control with chemicals and biocontrol agents. *Plant Dis* 102:1189–1217.
- Oliva J, Stenlid J, Martínez-Vilalta J (2014) The effect of fungal pathogens on the water and carbon economy of trees: implications for drought-induced mortality. *New Phytol* 203:1028–1035.
- Park J-H, Juzwik J (2014) *Ceratocystis smalleyi* colonization of bitternut hickory and host responses in the xylem. *For Pathol* 44:282–292.
- Pearce (1996) Antimicrobial defences in the wood of living trees. *New Phytol* 132:203–233.
- Pouzoulet J, Scudiero E, Schiavon M, Santiago LS, Rolshausen PE (2019) Modeling of xylem vessel occlusion in grapevine. *Tree Physiol* 39:1438–1445.
- Pouzoulet J, Rolshausen PE, Charbois R, Chen J, Guillaumie S, Ollat N, Gambetta GA, Delmas CEL (2020) Behind the curtain of the compartmentalization process: Exploring how xylem vessel diameter impacts vascular pathogen resistance. *Plant Cell Environ* 43:2782–2796.
- Rioux D, Nicole M, Simard M, Ouellette GB (1998) Immunocytochemical evidence that secretion of pectin occurs during gel (gum) and tylosis formation in trees. *Phytopathology* 88:494–505.
- Rioux D, Blais M, Nadeau-Thibodeau N, Lagacé M, DesRochers P, Klimaszewska K, Bernier L (2018) First extensive microscopic study of butternut defense mechanisms following inoculation with the canker pathogen *Ophiognomonia clavignenti-juglandacearum* reveals compartmentalization of tissue damage. *Phytopathology* 108:1237–1252.
- Rogiers SY, Greer DH, Moroni FJ, Baby T (2020) Potassium and magnesium mediate the light and CO₂ photosynthetic responses of grapevines. *Biology* 9:144. <https://doi.org/10.3390/biology9070144>.
- Salleo S, Nardini A, Lo Gullo MA, Ghirardelli LA (2002) Changes in stem and leaf hydraulics preceding leaf shedding in *Castanea sativa* L. *Biol Plant* 45:227–234.
- Schippers JHM, Schmidt R, Wagstaff C, Jing H-C (2015) Living to die and dying to live: the survival strategy behind leaf senescence. *Plant Physiol* 169:914–930.
- Schneider CA, Rasband WS, Eliceiri KW (2012) NIH Image to ImageJ: 25 years of image analysis. *Nat Methods* 9:671–675.
- Sun Q, Rost TL, Reid MS, Matthews MA (2007) Ethylene and not embolism is required for wound-induced tylose development in stems of grapevines. *Plant Physiol* 145:1629–1636.
- Sun Q, Rost TL, Matthews MA (2008) Wound-induced vascular occlusions in *Vitis vinifera* (Vitaceae): Tyloses in summer and gels in winter. *Am J Bot* 95:1498–1505.
- Sun Q, Sun Y, Walker MA, Labavitch JM (2013) Vascular occlusions in grapevines with pierce's disease make disease symptom development worse. *Plant Physiol* 161:1529–1541.
- Tränkner M, Jáklí B, Tavakol E, Geifus C-M, Cakmak I, Dittert K, Senbayram M (2016) Magnesium deficiency decreases biomass water-use efficiency and increases leaf water-use efficiency and oxidative stress in barley plants. *Plant Soil* 406:409–423.
- Trueba S, Théroux-Rancourt G, Earles JM, Buckley TN, Love D, Johnson DM, Brodersen C (2022) The three-dimensional construction of leaves is coordinated with water use efficiency in conifers. *New Phytol* 233:851–861.
- Van Leeuwen K, Destrac-Irvine A, Dubernet M, et al. (2019) An update on the impact of climate change in viticulture and potential adaptations. *Agronomy* 9:514. <https://doi.org/10.3390/agronomy9090514>.
- Venturas M, López R, Martín JA, Gascó A, Gil L (2014) Heritability of *Ulmus minor* resistance to Dutch elm disease and its relationship to vessel size, but not to xylem vulnerability to drought. *Plant Pathol* 63:500–509.
- Warton IW, Hui FKC (2011) The arcsine is asinine: the analysis of proportions in ecology. *Ecology* 92:3–10.
- Woo HR, Kim HJ, Nam HG, Lim PO, LIM PO (2013) Plant leaf senescence and death – regulation by multiple layers of control and implications for aging in general. *J Cell Sci* 126:4823–4833.
- Yadeta KA, Thomma BPHJ (2013) The xylem as battleground for plant hosts and vascular wilt pathogens. *Front Plant Sci* 4:97. <https://doi.org/10.3389/fpls.2013.00097>.
- Zimmermann MH (1979) The discovery of tylose formation by a viennese lady in 1845. *IAWA Bull* 2-3:51–56.